EXTREME shearography

Development of a high-speed shearography instrument for measurements of the surface strain components during an impact event

Anisimov, Andrei G.; Groves, Roger M.

DOI
10.1117/12.2318692

Publication date
2018

Document Version
Accepted author manuscript

Published in
Speckle 2018

Citation (APA)
Anisimov, A. G., & Groves, R. M. (2018). EXTREME shearography: Development of a high-speed shearography instrument for measurements of the surface strain components during an impact event. In L. R. Jaroszewicz, & M. Kujawinska (Eds.), *Speckle 2018: VII International Conference on Speckle Metrology* (Vol. 10834). Article 108340X SPIE. https://doi.org/10.1117/12.2318692

Important note
To cite this publication, please use the final published version (if applicable).
Please check the document version above.

EXTREME shearography: development of a high-speed shearography instrument for measurements of the surface strain components during an impact event

Andrei G. Anisimov*[a], Roger M. Groves[a]
[a]Aerospace Non-Destructive Testing Laboratory, Delft University of Technology,
Kluyverweg 1, 2629 HS, Delft, The Netherlands

ABSTRACT

This work presents the design and preliminary results of a high-speed shearography instrument in development for surface strain components measurements during an impact event. Composite materials are vulnerable to extreme dynamic loadings such as blade off events or foreign object damage as their mechanical properties are strain rate dependent. The development of new instruments to reconstruct extreme dynamic events will provide important insight into the understanding of the behaviour of composites. Shearography provides a quantitative measurement of the surface strain components with a high sensitivity as it is a non-contact interferometric technique. The current configuration of the shearography instrument realises measurements of the out-of-plane surface strain components during an impact using a double frame approach. The first experimental results reveal phase maps registered during an impact event with μs temporal resolution. Later the experimentally measured surface strain components will be used as input and validation data for new numerical and analytical models of the impact response of composites. The overall set of technical parameters of the developing shearography instrument makes it one of the most extreme applications of shearography for material characterisation.

Keywords: high-speed shearography, double-pulse shearography, flexural waves, impact, composite materials, surface strain

1 INTRODUCTION

Improving the impact response of composite materials is an important direction of the materials development towards safer and lighter aircrafts. Composite materials are vulnerable to extreme dynamic loadings such as blade off events or foreign object damage (hail, runway debris, bird strike)[1]. The development of new instruments to reconstruct extreme dynamic events and to measure failure parameters will provide important insight into the understanding of the behaviour of composites. The strain development during the impact is of particular interest for both materials modelling and testing researchers[2,3]. The shearography[4-6] (speckle pattern shearing interferometry) technique is used in this project as it provides a quantitative measurement of the surface strain components with a high sensitivity as a non-contact interferometric technique.

Previously shearography was actively used for NDT inspection of composite materials[5,7,8], mostly for defect detection, localisation and characterisation. A posterior inspection of impact damage has been reported in the case of low[9-11] and high-velocity impacts[12]. Shearography was already used for the experimental mechanics of composites at slow strain rates[5,13-15], but not during an impact event at high impact speeds and energies. Various solutions for the fast shearography have been reported which employed pulsed lasers with high-speed[16] or more often double frame cameras with a higher spatial resolution[17] (sensors with interline frame transfer). The double frame approach was used for a vibration analysis in a frequency range up to a few kHz[18-20], including transient vibrations[21,22] and impact-induced flexural waves at low impact energies[23,24]. Previously holographic techniques were used to capture the propagation of flexural waves during the impact with the classical (film) pulsed holography[25,26] and later with the electronic speckle pattern interferometry (ESPI) by introducing a carrier frequency[27]. Double pulse ESPI was actively used for the impact monitoring[28,29] and numerical comparison with the available finite element models[30,31].

This work presents the design and preliminary experimental results of the developing high-speed shearography instrument for surface strain components measurement during an impact event. The main criteria for the developing the instrument were derived by maximising the value of the expected results for the validation of numerical models – to

*a.g.anisimov@tudelft.nl; phone +31 15 27 83099; http://www.aerondt.tudelft.nl

measure in- and/or out-of-plane surface strain components at impact speeds up to 200 m/s with a temporal resolution up to sub-µs over the field of view of 100×100 mm.

The current configuration of the shearography instrument realises measurements of the out-of-plane surface strain components during the impact using the double frame approach. The first experimental results presented in this paper reveal phase maps during the impact corresponding to the surface deformation with a µs temporal resolution. In the future, the experimentally measured surface strain components over the field of view will be used as input and validation data for new numerical and analytical models of the impact response of composites.

The framework for this work is the "EXTREME Dynamic Loading – Pushing the Boundaries of Aerospace Composite Material Structures" Horizon 2020 project[32]. Within the project, the shearography data is fused with high-speed digital image correlation (DIC) and in-situ impact data from various fibre optics and piezo-electric sensors. This fusion uses the strong points of each technique to provide reliable experimental input for numerical and analytical models of composites.

2 HIGH-SPEED SHEAROGRAPHY

A schematic of the EXTREME shearography instrument is presented in Figure 1. A speckle pattern is produced by illuminating an object with an expanded laser beam. Interferograms are recorded with one or more cameras with shearing devices in two or more surface states: before and after the deformation. In this project, the object is deformed by the impact loading with a gas-gun using an impactor. The synchronisation is done in a real-time to obtain a reliable registration of the impact event. Given the fact that the pulsed illumination at µs time scale is possible with modern lasers that can deliver two or several sub-pulses[33], the main choice is of the camera architecture. A detailed comparison of the different approaches is done in Table 1.

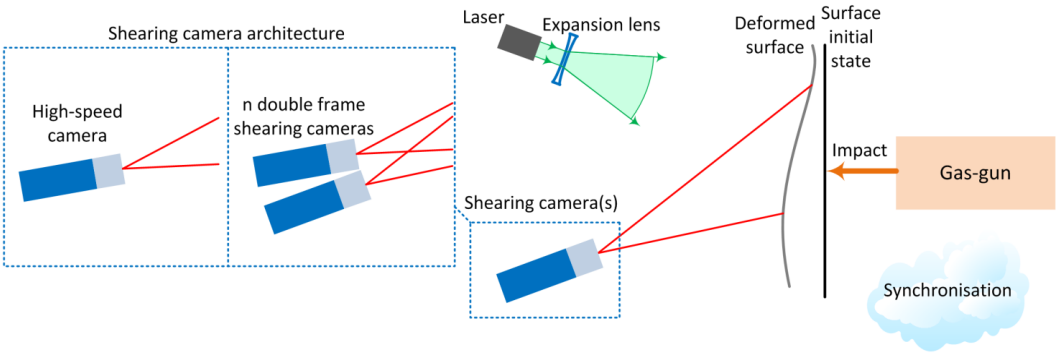

Figure 1. The EXTREME shearography instrument.

Table 1. Comparison of the shearing cameras architectures. All values depend on specific camera models.

Camera architecture	Main advantages	Main limitations
1. One or more high-speed cameras with a trade-off between the spatial resolution and the frame rate[34]	• Flexibility in various frame rates with a trade-off for the resolution • Ability to capture a sequence of interferograms to record the whole impact event with µs time step	• Low spatial resolution (order of 128×48 pixels) at frame rates close to 1 Mfps • Large pixel size (order of 20×20 µm) limiting the maximum spatial frequencies for the spatial phase shift
2. One or more high-speed cameras with a fixed resolution at extremely high frame rates (buffer on the sensor)[37,38]	• Moderate spatial resolution (close to 1 Mpixel) at extremely high frame rates (higher than 5Mfps) • Ability to capture a sequence of interferograms (up to 100-200 frames)	• High price, especially if 2 or 3 cameras are needed for the 3D shearography configuration[35,36]
3. One or more double frame cameras with an interline frame transfer[18-23,27-31]	• High spatial resolution (several Mpix) • Small pixel size (up to 3×3 µm) • Affordable price	• The number of frames is limited to 2 per camera • Long exposure time for the second frame if no extra shutter is used (equal to a readout time of the first frame, reaches 100-200 ms)

In this project, the third architecture with the double frame cameras was chosen due to high resolution and small pixel size in comparison with the high-speed cameras in options 1 and 2. The main limitation of two frames per camera can be overcome by increasing the number of cameras or by repeating the experiments with controlled delays[39]. The shearography configuration with spatial shifting[40] and the corresponding data processing flow is presented in Figure 2.

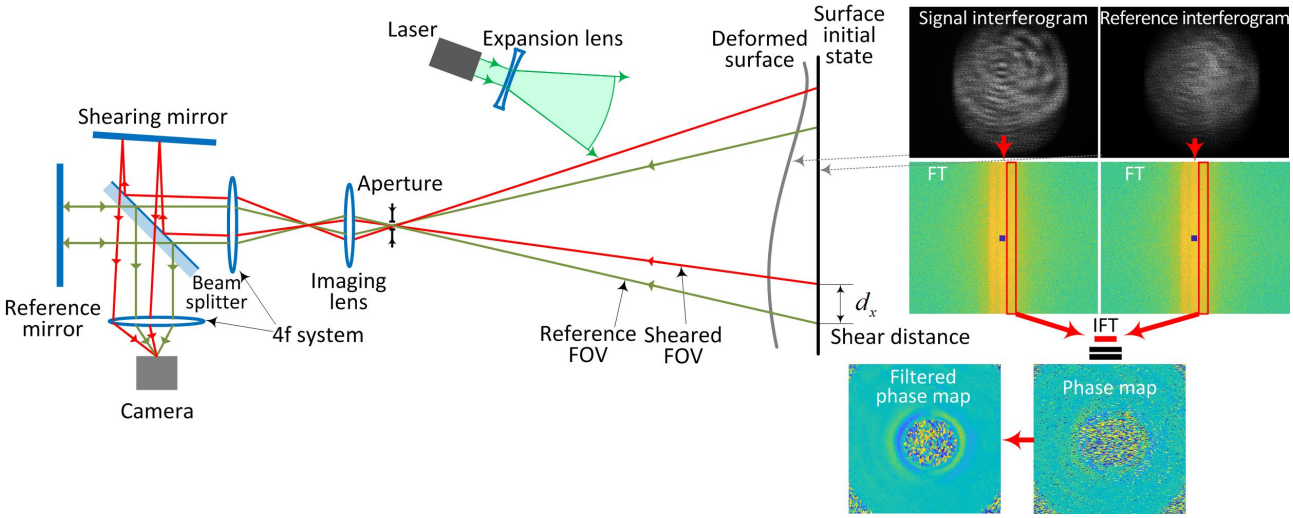

Figure 2. Schematic representation of the optical paths in the shearing device based on the modified Michelson interferometer with the data processing flow in the Fourier domain (FOV – field of view, FT – Fourier transform, IFT – inverse Fourier transform).

When the object surface is deformed, the change of the optical paths in the reference and sheared field of views causes a change of the phase $\Delta\phi_x$ at the camera, which can be extracted from complex amplitudes of the recorded interferograms. If the illumination and viewing directions are close to normal to the object, the phase change $\Delta\phi_x$ is a function of the out-of-plane surface strain component $\partial w/\partial x$ for the shear distance d_x in the x-direction:

$$\Delta\phi_x = \phi'_x - \phi_x^{ref} = \frac{4\pi}{\lambda}\partial w/\partial x\, d_x, \tag{1}$$

where ϕ'_x and ϕ_x^{ref} are the signal and reference phase differences obtained at the initial surface state and after the deformation, λ is the laser wavelength.

In case of the spatial phase shift with the 4f optical system used for an optical arrangement (Figure 2), an aperture or a slit acts as a low-pass filter that limits the frequency bandwidth of the recorded interferogram with the cut-off frequency[41] $f_c = D/2\lambda f$, where D is the aperture diameter or width of the slit, f is the focal length of the imaging lens.

The reference and the sheared beams interfere on the camera sensor at the shear angle which results in side maximums in the Fourier spectra that are shifted by the offset frequency[41] $f_o = \sin\beta/\lambda$, where β is the shear expressed in an angular form. After the inverse Fourier transformation, these side maximums yield a complex function that contains the phase information ϕ_x^{ref} and ϕ'_x for the interferograms captured before the deformation and after, respectively. In order to isolate these maximums, the offset frequency f_o has to be at least twice higher than f_c, which gives the well-known trade-off between the shear β, aperture D and the focal length f of the imaging lens:

$$f_o \le 2f_c \Rightarrow \frac{D}{f} \le \sin\beta. \tag{2}$$

The considerations below were also taken into account to optimise the performance of the developing instrument:

a) to decrease the shear distance d_x in Equation (1) to increase the dynamic range of the measuring strain $\partial w/\partial x$;

b) as a result of (a), to increase the focal length f and to decrease the aperture D (Equation (2)). However:

- both f and D define the speckle size Δs as $\Delta s = \lambda f/D$ which has to be more than 6 pixels[41];
- the desired field of view, the instrument geometry and the camera sensor size define the focal length f;
- the signal to noise ratio of the capturing interferograms affects the aperture D.

3 EXPERIMENTAL RESULTS

3.1 EXTREME shearography instrument

The current configuration of the shearography instrument (Figure 3) realises measurements of the out-of-plane surface strain components ($\partial w/\partial x$, $\partial w/\partial y$) during the impact using the double frame approach. Because of the gas-gun, a chamber design with 3 zones was made, driven by the safety measures:

a) an impact zone with the synchronisation unit providing a real-time information about the approaching impactor using a set of 20 optical interrupters placed one after another in a synchronisation unit (Figure 3 (a);
b) a monitoring zone where the back surface of the specimen is observed;
c) a shearography zone where the shearing camera and the laser beam path are placed.

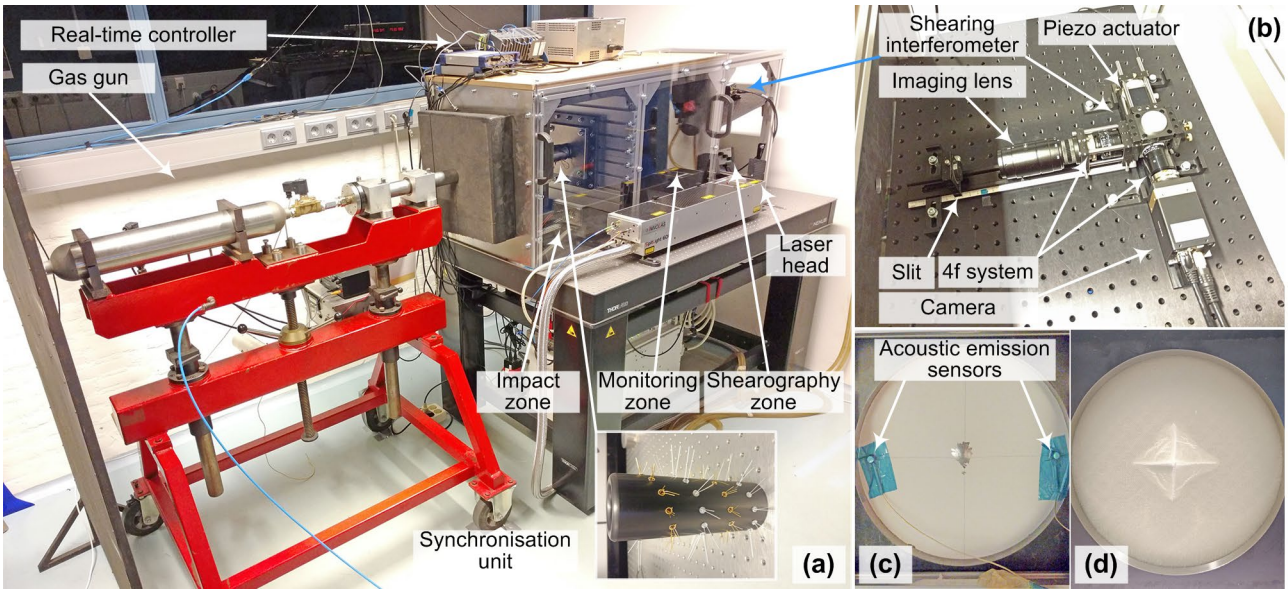

Figure 3. EXTREME shearography instrument: (a) the gas-gun and the impact chamber, (b) the shearography zone, (c, d) impacted metal and composite specimens, respectively.

The gas-gun is adapted for impact speeds up to 200 m/s. The gun operates under pressurised air or nitrogen and impact release is controlled by an electromagnetic valve. The impactor design with the tip with the radius of curvature of 5 mm was used following standard practice in industry for impact testing.

A double frame camera Bobcat B3420 by Imperx captures interferograms during the impact event by viewing through a shearing interferometer. The camera has an interline frame transfer with a resolution of 3388×2712 pixels, a pixel size of 3.69x3.69 μm and an interframing time of 200 ns. The speckle pattern is produced by a customised SpitLight 600-10 Nd:YAG-Lasersystem by InnoLas Laser GmbH with the wavelength of 532 nm illuminating the back surface of the specimen. Two portions of the single pulse with energy from 100 up to 500 mJ sequentially illuminate the object under control of a Pockels cell. The repetition rate of the main pulses is 10 Hz with the minimal sub-pulse separation of 1 μs.

A modified Michelson interferometer realises both the temporal phase shifting for the system calibration and the spatial one for the phase map registration during the impact. Temporal phase shifting and the shear are performed using a three coordinate piezo-electric actuator PSH 4z by Piezosystem Jena which is used in the shearing arm of the interferometer. The spatial phase shifting is based on a 4f system (two 50 mm Xenoplan lenses by Schneider) with a 0.4 mm slit in front of the imaging lens to achieve a better quality of the phase maps in comparison with a circular aperture[42].

The trade-off between the interferometer parameters (Equation (2)) was made as follows:

a) the shear distance d_x was set in the range of 3..4 mm and was later calibrated. A rational minimal value at the distance between the camera and the object of 600-700 mm was selected to avoid damage of the optics during the impact event;
b) the focal length was maximised up to 50 mm (LM50SC by Kowa);
c) a 0.4 mm slit was chosen as a rational compromise resulting in:

- deliberate 25% overlap of the central and side maximums of the Fourier spectra (with $f_c = 0.004/\lambda$ and $f_o = 0.007/\lambda$) decreasing the quality of the phase maps [the smaller the slit, the bigger the spectral separation];
- average speckle size of 16 pixels in the x-direction which limits the spatial resolution [the bigger the slit, the smaller the speckle, the higher the spatial resolution];
- high signal to noise ratio of the capturing interferograms [the bigger the slit, the more light is captured].

The shear distances in the x-direction were calibrated over the field of view by processing a checkerboard image captured first through the reference field of view, then through the sheared one. Shear distances for the x-direction were spatially determined in the range of 73.1±0.6 pixels in the image space and 3.47±0.03 mm on the specimen (range of 1 standard deviation).

3.2 "On-the-fly" synchronisation based on the approaching impactor

All parts of the instrument require reliable real-time synchronisation with an accuracy up to 1 µs to capture the initial moment of impact. The overall shooting procedure takes more than 5 seconds (Figure 4 (a)) and includes:

[phase 1] pre-heat of the laser for a thermal stabilisation (10..50 double pulses at 10 Hz);

[phase 2] shot (opening of the gas-gun valve);

[phase 3] travelling of the impactor towards the specimen being continuously monitored by the optical interrupters (including calculation of the expected time of arrival and well-timed triggering of the laser and the camera);

[phase 4] impact with capturing of two frames synchronously with two sub-pulses and acoustic emission signals.

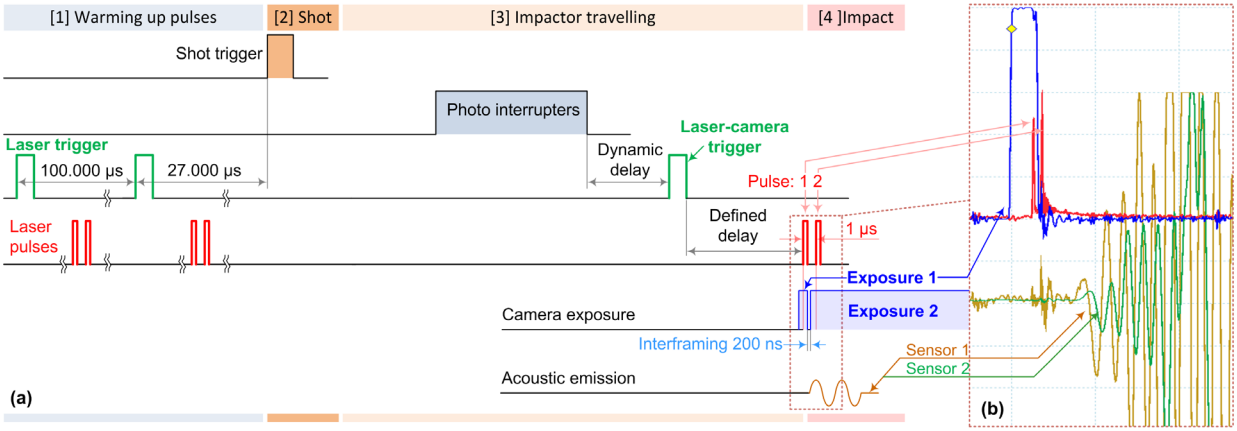

Figure 4. Timing of the shooting routine: (a) diagram with the main triggers and signals, (b) oscillogram captured during the impact.

"On-the-fly" synchronisation is done by processing signals from 20 optical interrupters which cross the path of the impactor using a real-time processing unit with an FPGA architecture. The actual speed of the impactor is calculated based on the relative delays between these 20 signals, then the appropriate delays to trigger the laser and the camera are calculated. The actual moment of impact is estimated by processing signals (brown and green in Figure 4 (b)) from two miniature acoustic emission sensors PICO HF-1.2 by Physical Acoustics operating in the range of 500-1850 kHz which are taped directly to the specimen symmetrically to the specimen center.

3.3 Experimental phase maps

For the first experiments, the phase maps corresponding to the out-of-plane surface strain component $\partial w/\partial x$ were captured during the impact on metal specimens (2 and 3 mm thick aluminium in Figure 5 and 6, respectively, 1.5 mm steel in Figure 7) with the shear in the x-direction. The impactor and the damages in the specimens are shown in Figure 8. In case of 2 mm aluminium, the indentation resulted in a full perforation without a penetration, for other specimens only a repeatable indentation was observed.

The phase maps reveal the evolution of $\partial w/\partial x$ during 1 µs with varying delay up to 6.3 µs starting from the moment of the impact. This delay was estimated with an accuracy of ±0.5 µs by matching the acoustic emission signals (Figure 4 (b)) with the laser pulses and the wave propagation delay from the impact location to the acoustic emission sensors (Figure 9). During the tests, the impactor speed was in the range of 58.5±0.6 m/s corresponding to 53±1 J impact (range of 1 standard deviation) with the impactor of 31 g.

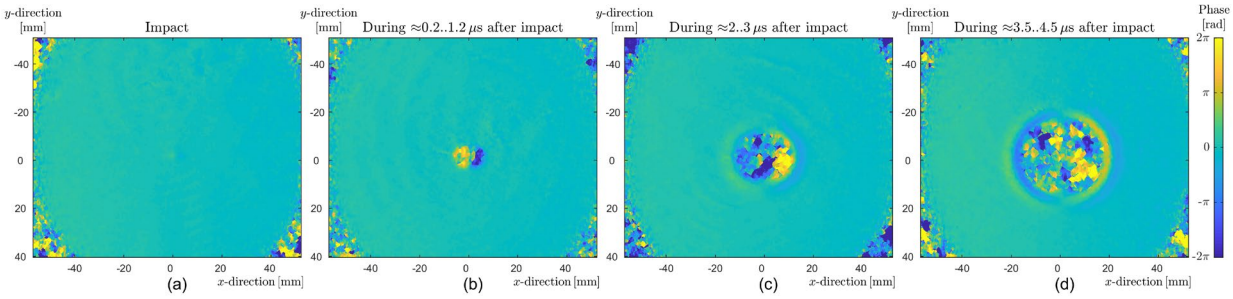

Figure 5. Phase maps corresponding to $\partial w/\partial x$, registered during the impact on 2 mm aluminium plate.

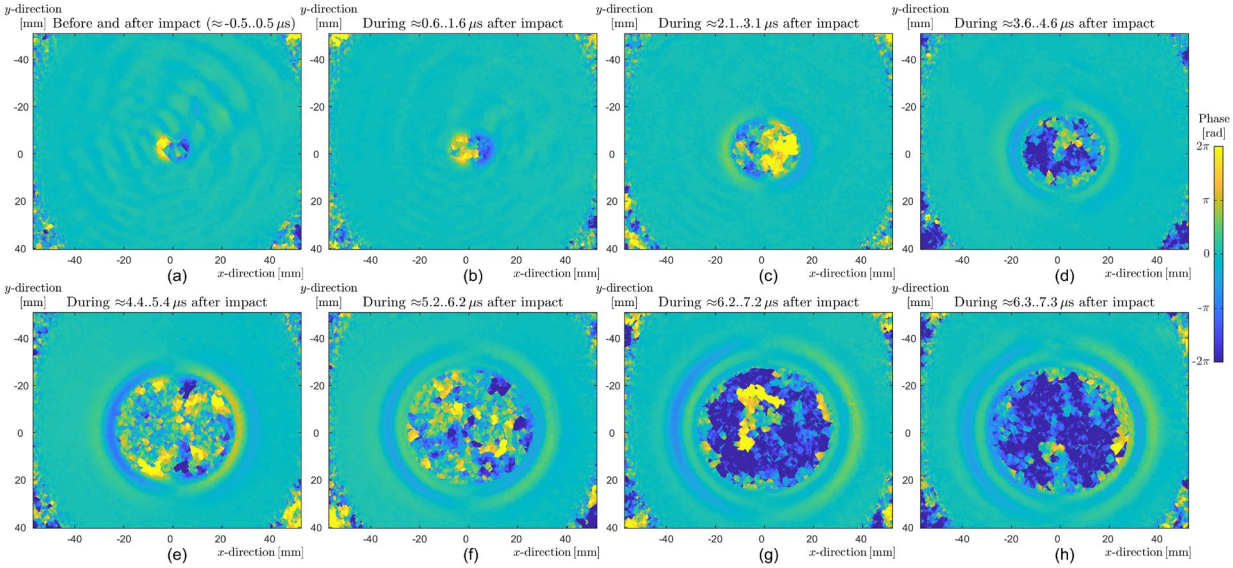

Figure 6. Phase maps corresponding to $\partial w/\partial x$, registered during the impact on 3 mm aluminium plate.

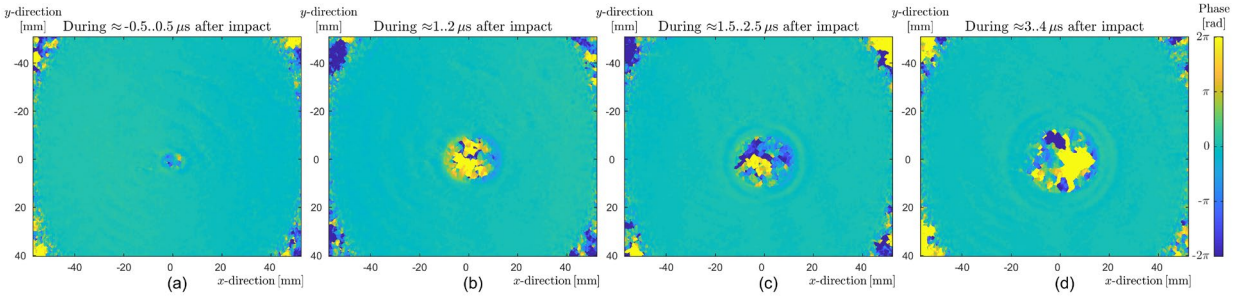

Figure 7. Phase maps corresponding to $\partial w/\partial x$, registered during the impact on 1.5 mm steel plate.

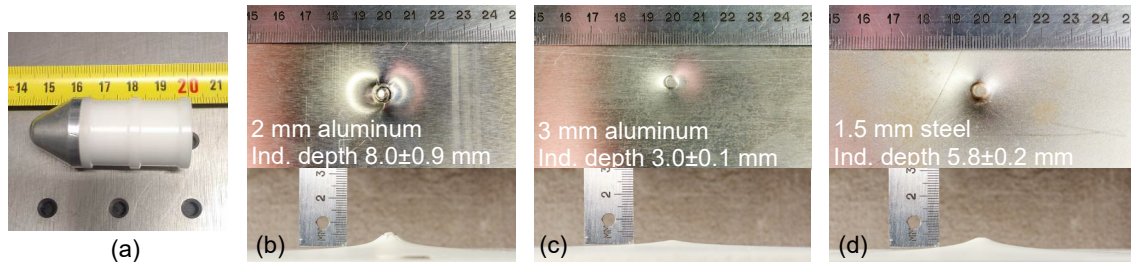

Figure 8. The impactor (a) and (b, c) the damaged zones in 2 and 3 mm aluminium and (d) 1.5 mm steel specimens. Indicated range of 1 standard deviation.

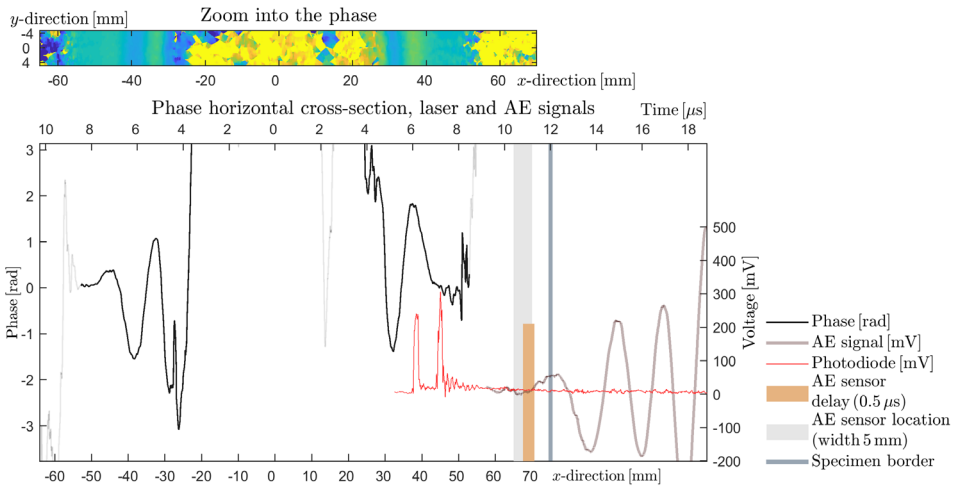

Figure 9. Matching the geometrical and time data: cross-section of the phase map taken after the impact (delay 6.3 μs, Figure 6 (h)) at the top-left and the signals from a photodiode and the acoustic emission (AE) sensor captured with an oscilloscope (bottom-right).

The phase cross-section in Figure 9 reveals the propagation of the flexural (longitudinal) wave after the impact (wavefront between -50..-40 and 40..50 mm). The top time axis is a function of the *x*-direction with an assumption that the wave velocity corresponds to speed of the longitudinal ultrasonic wave (6250 m/s for aluminium 2024-T4). The acoustic emission signal is matched with the sensor located in between 65 and 70 mm (grey area). An additional delay (brown area) of the sensor response of 0.5 μs was experimentally revealed by comparison of the time responses between the taped PICO HF-1.2 sensors and permanently bonded piezo-crystals.

The matching (Figure 9) reveals the overlap of the wavefront initiation at 45.6 mm (7.3 μs) with the second laser pulse detected with a photodiode. The remaining propagation time to the center of the sensor located at 67.5 mm is 3.5 μs, which results in the speed of 5475 m/s with a response delay of 0.5 μs. As mentioned earlier, the matching was done with an accuracy of ±0.5 μs which is a result of the geometrical uncertainties of the sensor positioning from a specimen to specimen (±1 mm), repeatability of the impact location (±2-3 mm) and the error of the moment of impact detection.

4 DISCUSSION

The first two phase maps in Figures 5-7 (a-b) reveal the out-of-plane deformation of the specimen during the first 1..2 μs after the impact, which is the initial response of the material to the impact loading. Further in time, starting from 2 μs the initiation of the flexural wave is observed (Figures 5-7 (c)). Remaining phase maps illustrate the propagation of the flexural ways at varying delays after the impact. The homogeneity of the metals results in a symmetric propagation of the waves. For the composites materials, it is expected to achieve an elliptical wavefront due to the anisotropy of the material properties[25,26].

The phase maps in Figures 5-7 with the flexural waves propagation will be used as one of several validation ways for the new numerical and analytical models developing within the EXTREME project[2,3,32]. For composites, this information about the early response may supplement the failure modes analysis (fibre or matrix fracture, delamination, plasticity). In the future, the in-plane surface strain components are of the particular interest for the material researcher, as the normal strains in *x*- and *y*-directions can be verified with alternative techniques as digital image correlation or strain gauges.

The main problem with the experimental phase maps is the loss of the correlation in the central parts of the impacted area. Several modifications are planned to overcome this issue, including:

a) use of a smaller slit and smaller shear distances together with testing of Mach-Zehnder interferometer[41];

b) increasing the laser wavelength from 532 nm to 1064 to double the dynamic range of the recording surface strain, also decreasing the speckle size from the current 16 pixels (along with the *x*-axis) up to 8, which is still sufficient for the correlation analysis with the practical suggestion of 6 pixels per speckle[41].

The choice of metals in the experiments was made to reduce the overall complexity and to test the instrument performance. The combination of the specimen weight and the impactor was chosen based on the mass criterion for the wave controlled impact response[1] where the mass ratio of the unclamped area of the specimen to the impactor should be

higher than 5. For the impact window of Ø150 mm and 31 g impactor the ratio is 3.2 and 4.7 for 2 and 3 mm aluminium, respectively, and 7.6 for 1.7 mm steel. This range of mass ratio was chosen because the observed dynamic wave-controlled impact is commonly caused by hail and runway debris causing barely visible damages in composites[1]. Later the same ratio will be used for the composite materials testing of similar thickness with a lighter impactor.

5 CONCLUSIONS

The design and preliminary results of the developing high-speed shearography instrument for the surface strain components measurements during an impact are presented. The current configuration of the shearography instrument realises measurements of the out-of-plane surface strain components ($\partial w/\partial x$, $\partial w/\partial y$) during the impact using the double frame approach. The technical parameters of the developing shearography instrument make it one of the most extreme applications of shearography for material characterisation. Future steps of the instrument development include optimisation of the interferometer to increase its dynamic range of the measuring strains, assessment of the in-plane surface strain components and recording of a sequence of interferograms (more than 2) in a "pulse train" regime.

ACKNOWLEDGEMENTS

The research on the high-speed shearography is funded by the H2020 project EXTREME, GA 636549.

REFERENCES

[1] Robin, O., "Mass criterion for wave controlled impact response of composite plates," Compos. Part A Appl. Sci. Manuf. 31(8) 879-887 (2000).
[2] Vignjevic, R., Djordjevic, N., De Vuyst, T. and Gemkow, S., "Modelling of strain softening materials based on equivalent damage force," Comput. Methods Appl. Mech. Eng. 335, 52-68 (2018).
[3] Giannaros, E., Kotzakolios, A., Sotiriadis, G., Tsantzalis, S. and Kostopoulos. V., "On fabric materials response subjected to ballistic impact using meso-scale modeling. Numerical simulation and experimental validation," Compos. Struct. 204, 745-754 (2018).
[4] Hung, Y. Y., "Shearography: a new optical method for strain measurement and non-destructive testing," Opt. Eng. 21, 213391 (1982).
[5] Steinchen, W. and Yang, L., [Digital Shearography], SPIE Press, Bellingham, Washington (2003).
[6] Francis, D., Tatam, R. P. and Groves, R. M., "Shearography technology and applications: a review," Meas. Sci. Technol. 21, 102001, 29 (2010).
[7] Hung, Y. Y., "Shearography for non-destructive evaluation of composite structures," Opt. Lasers Eng. 24(2-3), 161-182 (1996).
[8] Hung, Y. Y., "Applications of digital shearography for testing of composite structures," Compos. B Eng. 30(7), 765-773 (1999).
[9] Goto, D. T., Faraz, M. I., Rans, C. D. and Groves, R. M., "Low energy impact damage detection using shearography," Proc. Photomechanics (2011).
[10] Kim, G., Hong, S., Jhang, K. Y. and Kim, G. H., "NDE of low-velocity impact damages in composite laminates using ESPI, digital shearography and ultrasound C-scan techniques," Int. J Precis. Eng. Manuf. 13(6), 869-876 (2012).
[11] Ochôa, P., Infante, V., Silva, J. M. and Groves, R. M., "Detection of multiple low-energy impact damage in composite plates using Lamb wave techniques," Compos. B Eng. 80, 291-298 (2015).
[12] Okafor, A. C., Otieno, A. W., Dutta, A. and Rao, V. S., "Detection and characterization of high-velocity impact damage in advanced composite plates using multi-sensing techniques," Compos. Struct. 54(2-3), 289-297 (2001).
[13] Lee, J. R., Molimard, J., Vautrin, A. and Surrel, Y., "Application of grating shearography and speckle shearography to mechanical analysis of composite material," Compos. Part A Appl. Sci. Manuf. 35(7-8), 965-976 (2004).
[14] Lomov, S. V., Ivanov, D. S., Verpoest, I., Zako, M., Kurashiki, T., Nakai, H., Molimard, J. and Vautrin, A., "Full-field strain measurements for validation of meso-FE analysis of textile composites," Compos. Part A Appl. Sci. Manuf. 39(8), 1218-1231 (2008).
[15] Anisimov, A. G., Müller, B., Sinke, J. and Groves, R. M., "Analysis of thermal strains and stresses in heated fibre metal laminates," Strain 54, 1-16 (2017).

[16] Moore, A. J., Hand, D. P., Barton, J. S. and Jones, J. D. C., "Transient deformation measurement with electronic speckle pattern interferometry and a high-speed camera," Appl. Opt. 38, 1159-1162 (1999).
[17] Steinchen, W., Yang, L. X., Kupfer, G., Maeckel, P. and Voessing, F., "Toward double-pulse digital shearography," Proc. SPIE 3418 (1998).
[18] Spooren, R., Dyrseth, A. A. and Vaz, M., "Electronic shear interferometry: application of a (double-) pulsed laser," Appl. Opt. 32(25), 4719-4727 (1993).
[19] Chen, F., Luo, W. D., Dale, M., Petniunas, A., Harwood, P. and Brown, G. M., "High-speed ESPI and related techniques: overview and its application in the automotive industry," Opt. Lasers Eng. 40(5-6), 459-485 (2003).
[20] Francis, D., "Surface strain measurement using pulsed laser shearography with fiber-optic imaging bundles," PhD Thesis, Cranfield University, Cranfield, UK (2008).
[21] Pedrini, G., Pfister, B. and Tiziani, H., "Double pulse-electronic speckle interferometry," J. Mod. Opt. 40(1), 89-96 (1993).
[22] Pedrini, G. and Tiziani, H. J., "Double-pulse electronic speckle interferometry for vibration analysis," Appl. Opt. 33(34), 7857-7863 (1994).
[23] Shim, V. P. W., Toh, S. L. and Quah, S. E., "Impact-induced flexural waves in a Timoshenko beam – Shearographic detection and analysis," Exp. Mech. 34(4), 340-348 (1994).
[24] Santos, F., Vaz, M. and Monteiro, J., "A new set-up for pulsed digital shearography applied to defect detection in composite structures," Opt. Lasers Eng. 42(2), 131-140 (2004).
[25] Fällström, K-E., Gustavsson, H., Molin, N-E. and Wåhlin, A., "Transient bending waves in plates studied by hologram interferometry," Exp. Mech. 29(4), 378-387 (1989).
[26] Fällström, K-E., Lindgren, L-E. and Molin, N-E., "Transient bending waves in anisotropic plates studied by hologram interferometry," Exp. Mech. 29(4), 409-413 (1989).
[27] Schedin, S. and Gren, P., "Phase evaluation and speckle averaging in pulsed television holography," Appl. Opt. 36(17), 3941-3947 (1997).
[28] Field, J. E., Walley, S. M., Proud, W. G., Goldrein, H. T. and Siviour, C. R., "Review of experimental techniques for high rate deformation and shock studies," Int. J Impact Eng. 30(7), 725-775 (2004).
[29] Schmidt, A., "Experimental investigations on nondestructive testing methods for defect detection with double-pulse electronic speckle pattern interferometry," PhD Thesis, Helmut-Schmidt-University / University of the Federal Armed Forces, Hamburg, Germany (2009).
[30] Diaz, F. V. and Kaufmann, G. H., "Impact-induced transient deformation analysis by means of digital speckle pattern interferometry," Exp. Mech. 39(4), 311-316 (1999).
[31] Lopes, H., Guedes, R. M., Vaz, M. A. P. and Rodrigues, J. D., "Study of transient wave propagation in plates using double pulse TV holography," Proc. International Conference on Advances in Computational and Experimental Engineering and Sciences, 2216-2221 (2004).
[32] "EXTREME Dynamic Loading – Pushing the Boundaries of Aerospace Composite Material Structures," www.extreme-h2020.eu (28 August 2018).
[33] Nösekabel, E. H., Honsberg, W. and Kelnberger, R., "Development and application of a 10 Hz Nd:YAG double pulse laser for vibration measurements with double pulse ESPI," In Fringe 2009, 1-6, Springer, Berlin (2009).
[34] Helfrick, M. N., Niezrecki, C., Avitabile, P. and Schmidt, T., "3D digital image correlation methods for full-field vibration measurement," Mech. Syst. Signal Process. 25(3), 917-927 (2011).
[35] James, S.W. and Tatam, R.P., "3D shearography for surface strain analysis," Proc. SPIE 3783, 247 (1999).
[36] James, S.W. and Tatam, R.P., "Time-division-multiplexed 3D shearography," Proc. SPIE 3744, 394-403 (1999).
[37] Crooks, J., Marsh, B., Turchetta, R., Taylor, K., Chan, W., Lahav, A. and Fenigstein, A., "Kirana: a solid-state megapixel uCMOS image sensor for ultrahigh speed imaging," Proc. SPIE 8659, 865903 (2013).
[38] Jannotti, P. and Schuster, B. E., "Application of 3D digital image correlation in ballistic testing," J. Dynamic Behavior Mater. 1, 155-161 (2018).
[39] Wernet, M. and Opalski, A., "Development and application of a MHz frame rate digital particle image velocimetry system," In 24th AIAA Aerodynamic Measurement Technology and Ground Testing Conference, 2184 (2004).
[40] Yang, L. and Xie, X., [Digital Shearography: New Developments and Applications], SPIE Press, Bellingham, Washington (2016).
[41] Pedrini, G., Zou, Y. L. and Tiziani, H. J., "Quantitative evaluation of digital shearing interferogram using the spatial carrier method," Pure and Appl. Opt. A 5.3, 313 (1996).
[42] Xie, X., Li, J., Zhang, B., Yan, L. and Yang, L., "Improvement of phase map quality for Michelson interferometer based spatial phase-shift digital shearography," Asian J. Phys. 24(10), 1391-1400 (2015).